ACADEMIC PRESS

Available online at www.sciencedirect.com
SCIENCE DIRECT®

Journal of Catalysis 218 (2003) 375–385

JOURNAL OF CATALYSIS

www.elsevier.com/locate/jcat

Structure-activity relations for Ni-containing zeolites during NO reduction II. Role of the chemical state of Ni

B.I. Mosqueda-Jiménez,[a,b] A. Jentys,[a] K. Seshan,[b] and J.A. Lercher [a,*]

[a] *Institute of Chemical Technology, Technische Universität München, Lichtenbergstrasse 4, 85748 Garching, Germany*
[b] *Catalytic Processes and Materials, Faculty of Chemical Technology, University of Twente, PO Box 217, 7500 AE Enschede, The Netherlands*

Received 5 December 2002; revised 21 February 2003; accepted 24 February 2003

Abstract

The influence of the metal in Ni-containing zeolites used as catalysts for the reduction of NO with propane and propene was studied. In the fresh catalysts, Ni is located in ion exchange positions for Ni/MOR, Ni/ZSM-5, and Ni/MCM-22. The formation of carbonaceous deposits, the removal of Al from framework positions, and the migration of Ni ions to nonaccessible positions were identified as primary reasons for the changes in the activity of the catalysts during the reduction of NO with hydrocarbons. Changes in the chemical state of Ni, i.e., isolated Ni^{2+} species being converted into Ni^{2+} on the surface of small Ni oxide clusters, affect the activity to a less significant extent compared to the changes in the location of Ni within the zeolite framework.

Keywords: Hydrocarbon-SCR; Propene; Propane; Ni-exchanged zeolites; Structure; Infrared spectroscopy; XAS; NMR

1. Introduction

The reduction of nitric oxide with hydrocarbons using transition metal-exchanged zeolites represents an alternative for the use of NH_3 as reducing agent in the selective catalytic reduction of NO_x. Typically, transition metals such as Co [1–4], Fe [5–9], and Ni [2,3,10] supported on zeolites are investigated as potential catalysts for the reduction of NO using hydrocarbons as reductant [11].

Ni-exchanged zeolites have been found active for the reduction of NO with methane [2,3,10]. Witzel et al. prepared Ni catalysts by ion exchanging the sodium form of ZSM-5 with nickel acetate. Maximum NO conversions to N_2 of 90 and 75% were found during the reduction of NO with isobutane and methane, respectively [10].

Several authors have pointed out that the coordination of the metal ions at different cationic sites of the zeolites [12,13] may affect the relative diffusivities of the reactants or the activation of the hydrocarbon molecules [13–15]. Li and Armor [12] suggested that on ferrierite Co ions located in 8-membered rings are less active for NO reduction with methane than sites in 10-membered rings. Kaucký et al. [13] reported the influence of the location of Co cations in zeolites on the catalytic activity for the reduction of NO with methane. In general, α-type Co ions, bound to framework oxygens of the wall of the main channel, were found to be the most active Co ions in mordenite and ferrierite, while in ZSM-5 β-type Co ions, coordinated to the deformed six-membered ring at the intersection of straight and sinusoidal channels, possess the highest activity. It is suggested that the stabilization of isolated metal cations at short distances within the zeolite structure might be the reason for the high SCR activity of metal-exchanged zeolites [13]. In the case of FeZSM-5 a binuclear iron complex has been proposed as the active site for the reduction of NO with hydrocarbons [7,8,16].

The deactivation of catalysts during the reduction of NO with hydrocarbons might result either from the formation of carbonaceous deposits, which block the active sites [9,17, 18], or from changes in the catalyst structure. The formation of carbonaceous species was found to be more severe when unsaturated reducing agents (e.g., olefins) are used [17] and for highly acidic catalysts [18]. For alumina-supported Pt catalysts, metal sintering during NO reduction in the presence of excess oxygen at temperatures below 500 °C [18,19] was observed. The metal particles in Cu- [20–22] and Ag-exchanged zeolite catalysts [23] are known to sinter under

* Corresponding author.
E-mail address: johannes.lercher@ch.tum.de (J.A. Lercher).

0021-9517/03/$ – see front matter
doi:10.1016/S0021-9517(03)00146-5

the flow of the reaction mixture due to the presence of steam. In addition, deactivation of the zeolite-based catalysts due to removal of Al^{3+} from framework positions (dealumination) during the NO reduction with methane was observed for H-mordenite [24] and for Cu-ZSM-5 in the presence of H_2O due to the formation of inactive species such as copper aluminate [25]. Petunchi and Hall [22] reported for Cu-ZSM-5 at temperatures above 350 °C a severe deactivation of the catalysts resulting from dealumination.

The effect of the type and concentration of acid sites on the activity of Ni-exchanged MOR, ZSM-5, and MCM-22 zeolites was discussed in the first part of this study [26] and in Ref. [27]. It was shown that the higher activity of Ni-exchanged ZSM-5 is related to the high concentration and strength of the acid sites present in this material compared to MOR and MCM-22. The rate-limiting step was assigned to the activation of the alkane and to the subsequent formation of olefins by dehydrogenation on SiOHAl groups and on the Ni^{2+} ions. Oligomerization of hydrocarbons led to the formation of carbonaceous deposits on the three materials being more severe for the NO reduction with propene. A high concentration of acid sites was found to promote the formation of carbonaceous deposits, which resulted in a partial blocking of the pores. The material with the largest pore diameter (MOR) was deactivated to a lesser extent by coke formation compared to the other zeolite supports.

In this part, the role of Ni and of structural changes of the metal and the zeolite support on the catalytic properties of Ni-exchanged zeolites for NO reduction are discussed.

2. Experimental

2.1. Preparation of samples

Ni-exchanged MOR, ZSM-5, and MCM-22 were prepared by liquid phase ion exchange of the sodium form of the zeolites carried out from an aqueous solution of $Ni(NO_3)_2$ at 80 °C under continuous stirring for 24 h. Subsequently, the zeolite was separated from the ion exchange solution by centrifugation, washed thoroughly with deionized water, and dried overnight at 100 °C. The effect of the type and concentration of acid sites of these samples is described in Ref. [26]. Composition and acid site concentration of the samples are summarized in Table 1.

2.2. Characterization

The adsorption of CO was followed by IR spectroscopy, using a Bruker IFS-88 spectrometer equipped with a vacuum cell. Samples were pressed into self-supported wafers and activated at 500 °C for 60 min. The increase in temperature during the activation was done in steps at 150, 250, and 300 °C for 30 min using a ramp of 10 °C/min. Spectra of activated samples were recorded at 50 °C and CO was adsorbed at the same temperature using partial pressures from 1×10^{-3} to 1 mbar. To directly compare the spectra of the catalysts after the different pretreatment cycles all spectra were normalized by the intensity of the structural vibrations of the zeolite around 2000 cm^{-1}.

Table 1
Chemical composition of Ni-exchanged samples determined by AAS and acid site concentration measured by TPD [26]

Sample	Si/Al	Ni/Al	Na/Al	Ni loading (wt%)	Acid site concentration (mmol/g)
Ni/MOR	8.9	0.2	0.6	1.9	0.4
Ni/ZSM-5	16.4	0.4	0.3	2.0	0.7
Ni/MCM-22	12.3	0.2	0.0	1.8	0.8

^{27}Al-MAS-NMR spectra were measured on a Bruker MSL-300 NMR spectrometer at a field strength of 7.5 T and a spinning frequency of 15 kHz at a frequency of 78.205 MHz with 1.0 µs excitation pulses and recycle times of 0.1 s. The samples were pressed into 4 mm ZrO_2 rotors. The ^{27}Al chemical shifts were referenced to 1 M aqueous solution of $Al(NO_3)_3$ ($\delta = 0.0$ ppm).

X-ray absorption spectra were measured at HASYLAB, DESY (Hamburg, Germany) on beam line X1 using the Si (111) monochromator. The intensity of higher order reflections was minimized by detuning the second crystal of the monochromator to 60% of the maximum intensity. The samples were prepared as self-supporting wafers having a total absorption of 2.5 to optimize the signal to noise ratio. Fresh samples were activated in situ at 600 °C for 1 h in a stainless-steel cell. X-ray absorption spectra were recorded at the Ni edge (8333 eV) and analyzed with WINXAS97 software [28]. The local environment of the Ni atoms was determined from EXAFS using phase-shift and amplitude functions for Ni–O and Ni–Ni calculated assuming multiple scattering processes (FEFF Version 8.10) [29].

2.3. Catalytic measurements

The catalytic activity of the samples was studied in a continuous flow system with a fixed bed quartz reactor of 4 mm inner diameter containing 0.1 g of catalyst (particle size 300 µm). The reactant gas feed contained 1000 ppm of NO, 1000 ppm of C_3H_6 or C_3H_8, 5% O_2, and He as the carrier gas. A total flow of 50 ml/min, resulting in a space velocity of 20,000 h^{-1}, was used. The reaction products were analyzed by a chemiluminescence analyzer (TEI 42C) and a gas chromatograph (HP) equipped with a TCD detector using a mol sieve column for separation of N_2, O_2, and CO and a Porapak column for N_2O, C_3H_6, C_3H_8, and CO_2 analysis. Before the reaction, the catalysts were pretreated in situ under helium flow at 600 °C for 1 h.

The activity and the deactivation of the catalysts during the reaction were investigated by an extended procedure consisting of three cycles. In the first cycle the activity was followed at temperatures between 150 and 600 °C in intervals of 25 °C (cycle 1). This cycle was followed immediately by

cycle 2, where the activity was measured during the decrease of the temperature between 600 and 150 °C at intervals of 25 °C. Subsequently, the samples were treated in oxygen at 600 °C for 1 h followed by a third cycle between 150 and 600 °C with intervals of 25 °C (cycle 3). During all cycles the activity was followed at each temperature for 2 h.

3. Results

3.1. Changes in activity after NO reduction

As reported in Part I [26], the catalytic activities of the three Ni-containing catalysts decreased in the order Ni/ZSM-5 > Ni/MOR > Ni/MCM-22 for NO reduction with propane and Ni/MOR > Ni/ZSM-5 > Ni/MCM-22 for NO reduction with propene. The activities of the catalysts for the reduction of NO with propane during the three temperature cycles are compared in Fig. 1. For all catalysts, the temperature at which the maximum NO conversion was reached increased after the first cycle, while the variations of the activity with the reaction temperature during the second and third cycle was nearly identical. For Ni/MOR and Ni/ZSM-5 the same level of NO conversion was reached in all cycles, i.e., 69 and 80%, respectively, while for Ni/MCM-22 a significant decrease from 51 to 39% in the maximum conversion was observed after the first cycle. In the case of Ni/MOR, changes in the activity were apparent at temperatures above 325 °C, while for Ni/ZSM-5 and Ni/MCM-22 the differences in NO conversion were already noted above 175 °C. The smallest differences between the first and the second temperature cycle were observed for Ni/MOR. The selectivity to nitrogen-containing products was, however, not affected by the temperature cycles.

When propene was used as the reducing agent, marked coke formation occurred with Ni/ZSM-5 and Ni/MCM-22 [26]. With these catalysts, the variations of the activity during the second and third temperature cycle during the reduction of NO with propene, as shown in Fig. 2, are tentatively attributed to this pronounced coke formation. In contrast, the changes in the activity with Ni/MOR were independent of the type of reducing agent and similar to those during the reduction with propane. Thus, the activity of Ni/MOR during the second and third cycle was identical at temperatures above 400 °C during the reduction with propene.

The differences in the activity observed between the first and the subsequent cycles indicate that irreversible changes took place in the materials during the first temperature increase in the presence of reactive substrates. In order to determine the temperature at which structural changes occur, the NO reduction with propane was studied for Ni/MOR and Ni/ZSM-5 during extended time at constant temperature as shown in Fig. 3. For Ni/ZSM-5 (Fig. 3A) the conversion of NO at 475 °C increased from 83% at 1 h to 88% after 48 h, while the selectivities of nitrogen products did not change

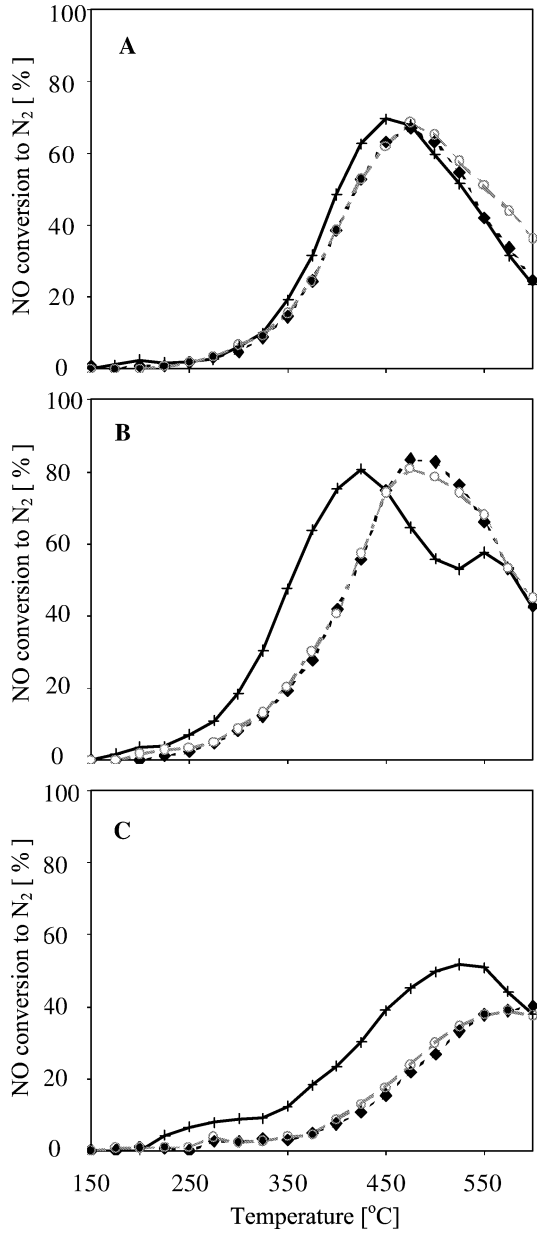

Fig. 1. NO conversion to N_2 during NO reduction with propane (+) ramp upward 1, (◆) ramp downward 1, (○) ramp upward 2 on (A) Ni/MOR, (B) Ni/ZSM-5, and (C) Ni/MCM-22.

during this time. After increasing the temperature to 600 °C, NO conversion decreased to 42% and finally reached 59% during a period of 10 h. Initially, small concentrations of NO_2 were observed; however, after 10 h the selectivity improved and N_2 was the only nitrogen-containing product. The formation of CO_2 decreased with time on stream and that of CH_4 increased. After 48 h of reaction at 600 °C, the temperature was reverted to 475 °C. Then, the conversions of NO and propane were much lower than those obtained with the fresh sample, i.e., 60 and 45%, respectively, while the selectivity to CO was much higher. Conversion and selectivity were stable during the following 24 h at 475 °C. After a subsequent temperature increase to 600 °C the same conversion

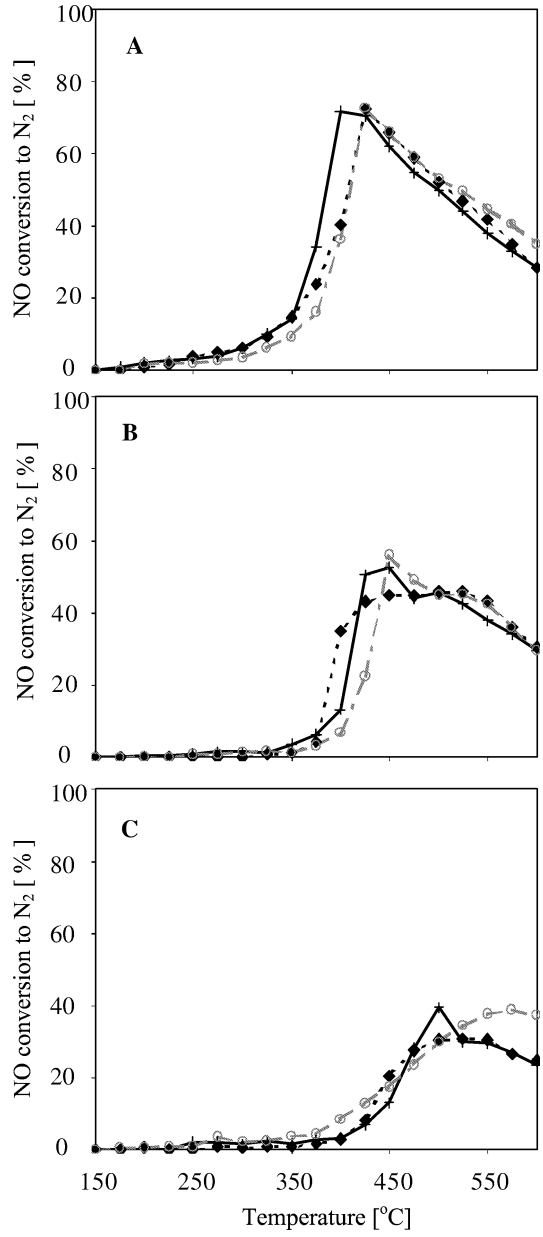

Fig. 2. NO conversion to N_2 during NO reduction with propene (+) ramp upward 1, (◆) ramp downward 1, (○) ramp upward 2 on (A) Ni/MOR, (B) Ni/ZSM-5, and (C) Ni/MCM-22.

and selectivity was observed as during the first experiments at 600 °C.

For Ni/MOR (Fig. 3B) only small variations in the conversions and selectivities were observed for the fresh catalyst for the reaction of NO with propane at 475 °C for 48 h, i.e., NO and propane conversion decreased from 70 to 68% and from 64 to 60%, respectively. After the temperature was increased to 600 °C the NO conversion initially decreased to 41% and reached during the subsequent 30 h 39%, passing through a minimum of 37%. After the stepwise change in temperature small concentrations of NO_2 were formed during the first hours, while after a longer time on stream N_2 became the only nitrogen product being detected.

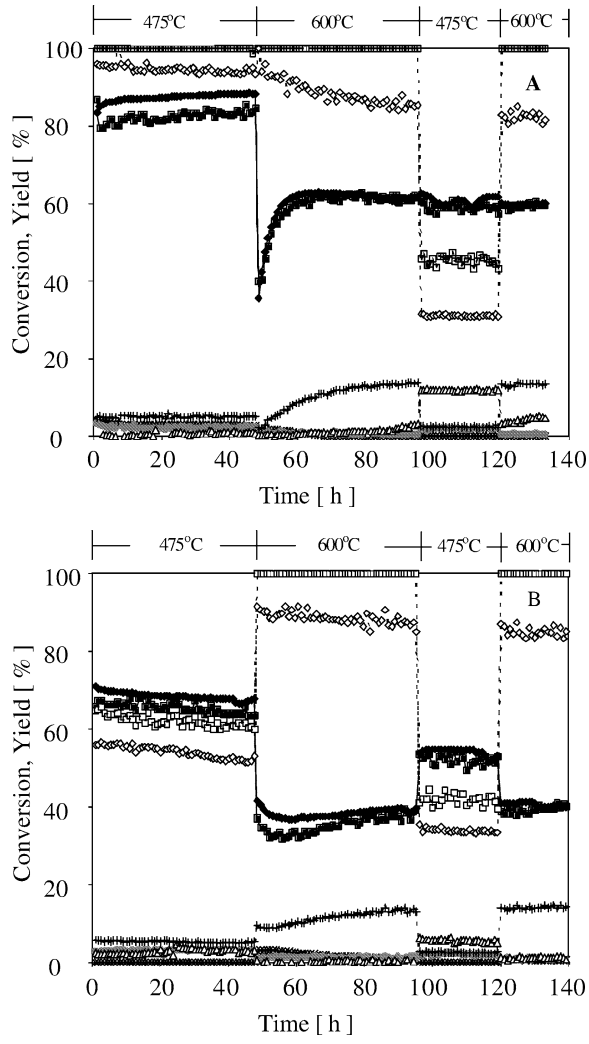

Fig. 3. Long-term reduction of NO with propane on (A) Ni/ZSM-5 and (B) Ni/MOR. Conversion of NO (◆) and propane (□), and yields of N_2 (■), N_2O (●), NO_2 (×), CO_2 (◇), CO (△), and CH_4 (+) at 475 and 600 °C.

In addition, the selectivity of the carbon-containing products changed significantly during this period. Similarly to Ni/ZSM-5, the amount of CO_2 formed decreased with time, while the amount of CH_4 formed increased. However, the changes observed for Ni/MOR were less pronounced than those reported for Ni/ZSM-5 above. After 48 h of reaction at 600 °C, the temperature was lowered to 475 °C and the NO conversion reached 54%, which was slightly lower than the conversion of the fresh catalyst (68%), and remained constant for the following 24 h. After an increase to 600 °C the conversions and selectivities reached the same levels as during the first cycle at 600 °C.

3.2. Characterization

The ^{27}Al-NMR spectra of the freshly activated catalysts and of the catalysts after NO reduction with propane and propene are shown in Fig. 4. For all samples a signal at 52 ppm, assigned to Al located in tetrahedral positions, was

observed [6,24]. For Ni/MCM-22 an unresolved asymmetric doublet, which corresponds to different framework sites, was observed [30–32]. For Ni/MCM-22 and for all samples after catalytic reduction of NO with propane and propene, a signal was observed near 0 ppm, which is assigned to Al in octahedral positions. This indicates the presence of extraframework Al-oxide species [6,24] formed during the calcination of the sample (Ni/MCM-22) [30–33] and during NO reduction. In addition, the change in the shape of the doublet at approximately 50 ppm for MCM-22 is associated with the dealumination of the zeolite [33]. Table 2 summarizes the fraction of Al present in octahedral positions in fresh samples and samples after the reduction of NO with propane and propene. The level of dealumination seems to be directly related to the catalyst activity. For Ni/MOR, which was slightly more active for the reduction of NO with propene compared to propane, a larger fraction of Al in octahedral positions was found for the samples after the NO reduction with propene. In contrast, for Ni/ZSM-5 and Ni/MCM-22 a higher activity and a higher fraction of Al in octahedral positions was observed for the NO reduction with propane.

Table 2
Fraction of Al present in octahedral position

Sample	Fraction of Al in octahedral position (%)
Ni/MOR fresh	0.0
Ni/MOR (propene)[a]	4.6
Ni/MOR (propane)[b]	2.4
Ni/ZSM-5 fresh	0.7
Ni/ZSM-5 (propene)[a]	2.4
Ni/ZSM-5 (propane)[b]	3.3
Ni/MCM-22 fresh	4.7
Ni/MCM-22 (propene)[a]	5.6
Ni/MCM-22 (propane)[b]	6.1

[a] After the reduction with propene.
[b] After the reduction with propane.

The IR spectra (region of the hydroxyl groups) of the activated catalysts and after NO reduction with propane and propene are shown in Fig. 5. The bands observed at 3745, 3680, and 3610 cm^{-1} correspond to terminal Si–OH groups, Al–OH groups on extraframework Al-oxide species, and bridging SiOHAl groups (Brønsted acid sites), respectively [34–37]. In general, the intensity of the band at 3610 cm^{-1} decreased after the reaction for all samples. The integral in-

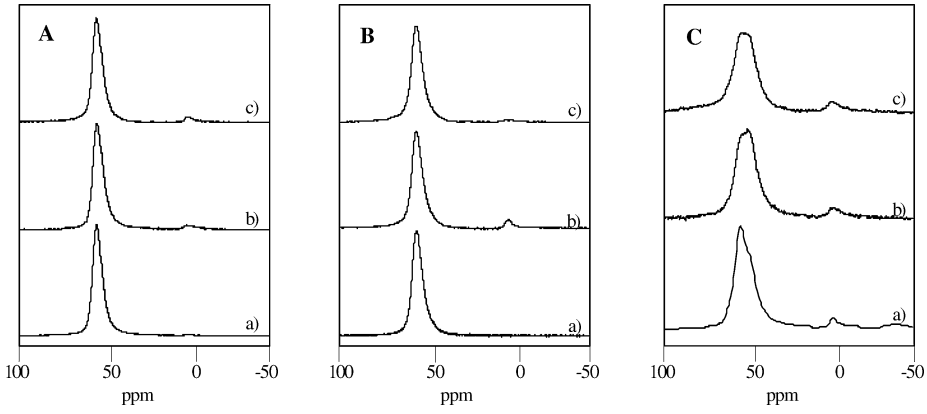

Fig. 4. ^{27}Al NMR spectra of fresh (a) and used samples collected after third reaction cycle, i.e., after reduction of NO with propene (b) and with propane (c) for Ni/MOR (A), Ni/ZSM-5 (B), and Ni/MCM-22 (C).

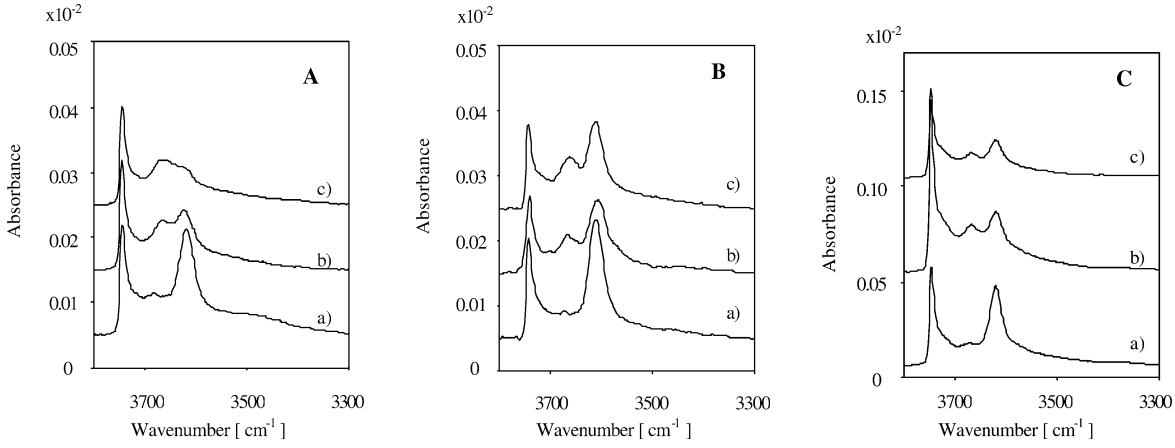

Fig. 5. Infrared spectra after activation of fresh (a) and used samples collected after third reaction cycle, i.e., after reduction of NO with propene (b) and with propane (c) for Ni/MOR (A), Ni/ZSM-5 (B), and Ni/MCM-22 (C).

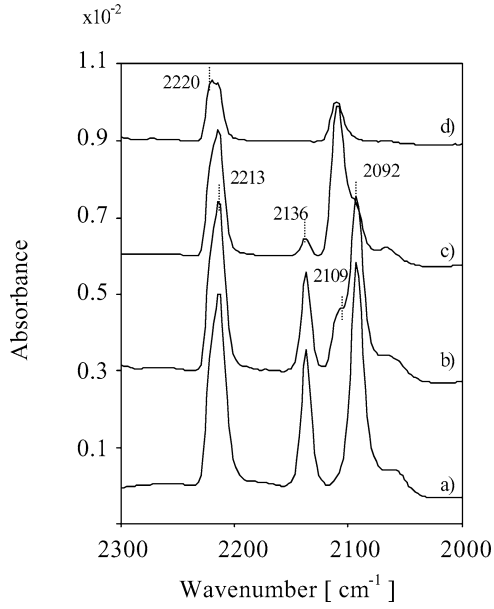

Fig. 6. Infrared spectra of CO adsorption on fresh Ni/ZSM-5 at 50 °C, at 1 mbar (a), 1×10^{-1} mbar (b), 1×10^{-2} mbar (c), and 1×10^{-3} mbar (d).

tensity of the band of the bridged hydroxyl groups decreased between 32 and 93% after reaction in comparison with the spectra of the fresh samples. The band at 3680 cm^{-1}, however, was more intense compared to the fresh samples. Changes in the intensity of the band at 3745 cm^{-1} were not observed.

The IR spectra during adsorption of CO at partial pressures between 1 and 10^{-3} mbar on Ni/ZSM-5 are shown in Fig. 6. At a CO partial pressure of 1 mbar bands at 2213, 2136, and 2092 cm^{-1} and a shoulder at 2220 cm^{-1} were observed. The IR bands at 2220 and 2213 cm^{-1} were assigned to Ni^{2+}–CO species [38]. The bands at 2136 and 2092 cm^{-1} were assigned to the symmetric and asymmetric stretching vibrations of dicarbonyl species on Ni^{+} ions, Ni^{+}–$(CO)_2$ [38–41]. At a CO partial pressure of 0.1 mbar the intensities of the bands at 2220, 2213, 2136, and 2092 cm^{-1} decreased. In addition, a new band at 2109 cm^{-1}, which was assigned to monocarbonyl species, Ni^{+}–CO [38–41], was observed. This band reached a maximum in intensity at a CO partial pressure of 10^{-2} mbar and decreased at 10^{-3} mbar. At this partial pressure the bands at 2092 and 2136 cm^{-1} were not observed. This indicates that with decreasing CO partial pressure Ni dicarbonyl species are replaced by monocarbonyl species followed by the desorption of CO. The presence of Ni^{+}–CO and Ni^{+}–$(CO)_2$ species is in line with the reduction of Ni^{2+} to Ni^{+} by dehydration in vacuum at temperatures above 300 °C as previously reported [41,42]. When the temperature is increased very slowly [43], water removed from the sample reduces Ni, according to Eq. (1) [41].

$$2Ni^{2+} + H_2O \xrightarrow{\Delta} 2Ni^{+} + 2H^{+} + \tfrac{1}{2}O_2. \quad (1)$$

The IR spectra during the adsorption of CO at 10^{-2} mbar on the fresh catalysts and on the catalysts after reduction of NO with propene and propane are shown in Fig. 7. For the fresh Ni/MOR (Fig. 7A) the intensity of the band at 2108 cm^{-1} (Ni^{+}–CO) was lower compared to Ni/ZSM-5 and Ni/MCM-22 and was not present in the spectra after the reaction. For the fresh Ni/ZSM-5 (Fig. 7B), two different Ni^{2+}–CO species at 2220 and 2213 cm^{-1} were observed, while for the samples after reaction only the band at 2213 cm^{-1} was present. In addition, Ni^{+}–CO species were clearly observed for the fresh Ni/ZSM-5, while after NO reduction with propene the intensity of the corresponding bands was very weak and the bands were absent for the sample after NO reduction with propane. In the spectra for Ni/MCM-22 after NO reduction with propane and propene (Fig. 7C) the intensity of the bands at 2113 and

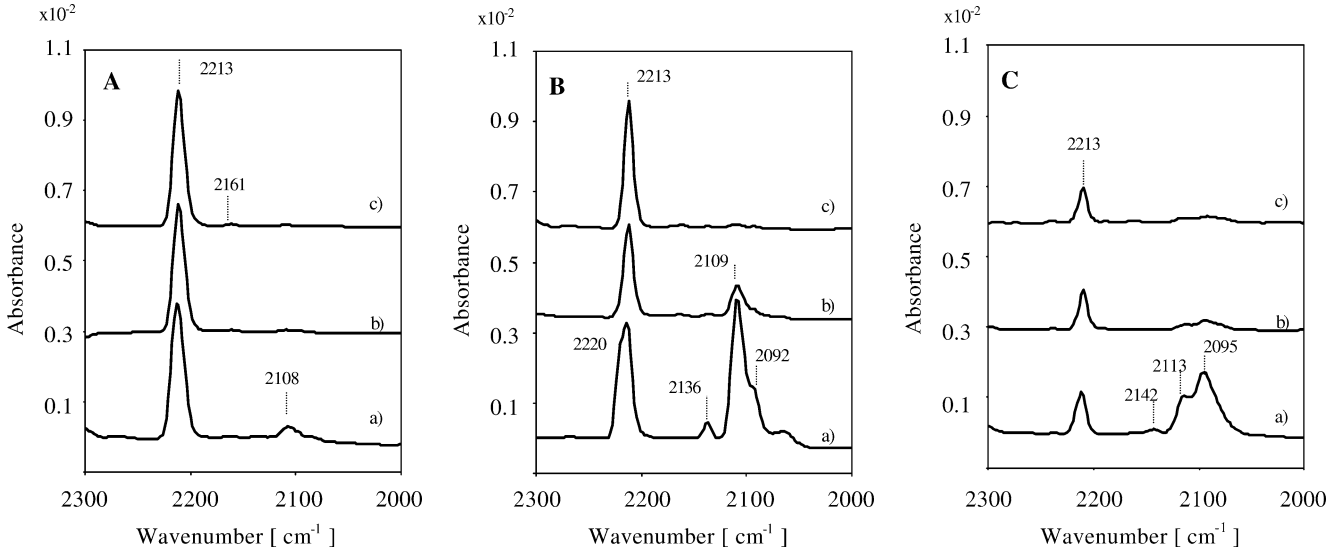

Fig. 7. Infrared spectra of CO adsorption at 1×10^{-1} mbar on fresh (a) and used samples collected after the third reaction cycle, i.e., after reduction of NO with propene (b) and with propane (c) for Ni/MOR (A), Ni/ZSM-5 (B), and Ni/MCM-22 (C).

Table 3
Decrease of the area of the bands of adsorbed CO at 0.1 mbar for samples after the reduction of NO with propane and propene in comparison with fresh samples

Sample	Decrease of accessibility of isolated Ni ions (%)
Ni/MOR (propene)[a]	34
Ni/MOR (propane)[b]	31
Ni/ZSM-5 (propene)[a]	57
Ni/ZSM-5 (propane)[b]	72
Ni/MCM-22 (propene)[a]	66
Ni/MCM-22 (propane)[b]	67

[a] After the reduction with propene.
[b] After the reduction with propane.

Table 4
Energy position of the Ni K-edge of Ni samples

Sample	Edge position half-height[c]	
	eV	Δ eV
Ni foil	8339.5	
NiO	8342.2	2.7
Ni/MOR fresh	8342.1	2.6
Ni/MOR (propene)[a]	8343.2	3.7
Ni/MOR (propane)[b]	8343.2	3.7
Ni/ZSM-5 fresh	8342.2	2.7
Ni/ZSM-5 (propene)[a]	8343.2	3.7
Ni/ZSM-5 (propane)[b]	8343.3	3.8
Ni/MCM-22 fresh	8342.3	2.8
Ni/MCM-22 (propene)[a]	8343.5	4.0
Ni/MCM-22 (propane)[b]	8343.2	3.7

[a] After the reduction with propene.
[b] After the reduction with propane.
[c] The energy corresponds to the absorption at half-height of the edge; i.e., absorbance = 0.5 in the normalized spectra.

2095 cm^{-1}, corresponding to CO interacting with Ni^{+}, was much lower in comparison with the fresh sample, while the band at 2213 cm^{-1} was not affected by the state of the sample. In general, for all samples studied the intensity of the bands assigned to CO interacting with Ni^{2+} ions was almost the same, when comparing fresh and used samples, while IR bands resulting from the adsorption of CO on Ni^{+} were much lower for the catalyst studied after the NO reduction. The area of the bands of CO adsorbed on Ni^{+} and Ni^{2+} at 0.1 mbar in the samples after reaction was integrated. We assumed that the molar extinction coefficients of these species are comparable and calculated the percentage of decreased area in comparison with fresh samples. The results are summarized in Table 3.

The energies of the Ni K X-ray absorption edge, which can be related to the average charge of the Ni atoms in the samples, are summarized in Table 4. For the fresh samples and for NiO a shift in the edge position of +2.7 eV with respect to metallic Ni was observed. After the reaction, the energy of the Ni K-edge of the samples increased by +3.8 eV.

The magnitude of the Fourier transformed EXAFS (weighted with k^2) of the samples before and after the reduction of NO with propane and propene are compared in Fig. 8 and the results of the analysis of the EXAFS are summarized in Table 5. In principle, two contributions of Ni-oxide species at 1.6 and 2.5 Å, assigned to Ni–O and to Ni–Ni, were observed in all samples. In the fresh samples mainly Ni–O contributions were present and the low number of O neighbors ($N_{Ni-O} \sim 3$), the absence of Ni–Ni contributions ($N_{Ni-Ni} < 0.8$), and the slightly shorter distance between Ni and O compared to Ni-oxide indicates that the Ni ions are mainly located on ion exchange positions. After the NO reduction a significant increase in the Ni–Ni and to a lesser extent in the Ni–O contributions was observed, which points to the formation of larger Ni-oxide species on Ni/MOR and Ni/ZSM-5 during the reaction. In contrast, for Ni/MCM-22 only Ni–O contributions, similar to the fresh samples, were observed after the reaction. Table 6 summarizes the size of the NiO clusters formed after the reduction of NO with propane and propene. The size of the clusters was estimated from the coordination numbers using a series of NiO model clusters of different sizes with bulk phase geome-

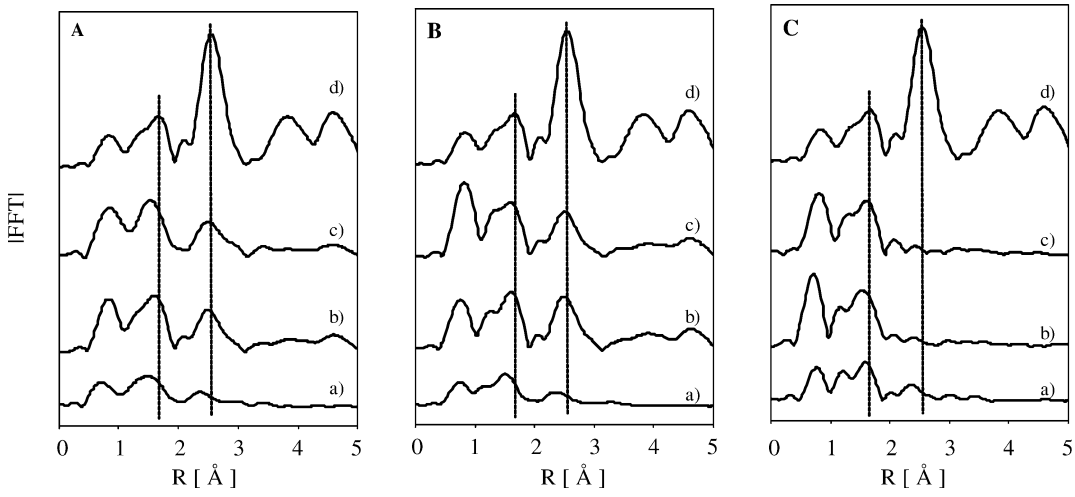

Fig. 8. Magnitude of the Fourier transformed oscillation (k^2 weighted) of fresh (a) and used samples collected after third reaction cycle, i.e., after reduction of NO with propene (b) and with propane (c) for Ni/MOR (A), Ni/ZSM-5 (B), and Ni/MCM-22 (C). NiO included as reference (d).

Table 5
Coordination parameters for Ni-exchanged zeolites determined by X-ray absorption spectroscopy

Sample	Ni–O			Ni–Ni		
	N	R (Å)	$\Delta\sigma^2$ (Å^2)	N	R (Å)	$\Delta\sigma^2$ (Å^2)
Ni foil				12	2.488	
NiO	6	2.084		12	2.947	
Ni/MOR fresh	2.95	2.020	0.0072	0.79	2.958	0.0034
Ni/MOR (propene)[a]	4.63	2.052	0.0043	4.81	2.951	0.0062
Ni/MOR (propane)[b]	4.51	2.052	0.0026	4.18	2.935	0.0053
Ni/ZSM-5 fresh	2.81	2.005	0.0072	0.73	2.958	0.0074
Ni/ZSM-5 (propene)[a]	4.22	2.054	0.0025	4.45	2.945	0.0039
Ni/ZSM-5 (propane)[b]	4.67	2.056	0.0044	3.91	2.954	0.0038
Ni/MCM-22 fresh	3.16	2.024	0.0072	0.68	2.843	0.0034
Ni/MCM-22 (propene)[a]	3.91	2.036	0.0022	–	–	–
Ni/MCM-22 (propane)[b]	3.34	2.043	0.0013	–	–	–

[a] After the reduction with propene.
[b] After the reduction with propane.

Table 6
Size of NiO clusters in samples after the reduction of NO with propane and propene

Sample	Size of cluster (Å)
Ni/MOR fresh	0
Ni/MOR (propene)[a]	8.0
Ni/MOR (propane)[b]	7.0
Ni/ZSM-5 fresh	0
Ni/ZSM-5 (propene)[a]	7.4
Ni/ZSM-5 (propane)[b]	6.5
Ni/MCM-22 fresh	0
Ni/MCM-22 (propene)[a]	0
Ni/MCM-22 (propane)[b]	0

[a] After the reduction with propene.
[b] After the reduction with propane.

try. From these model clusters the average Ni–O and Ni–Ni coordination numbers were calculated as a function of the cluster size and used to estimate the size of the NiO clusters on the zeolite samples. The size of the clusters of NiO formed in Ni/MOR and Ni/ZSM-5 after the reduction of NO with propane and propene ranges from 6.5 to 8 Å.

4. Discussion

In principle two reasons, i.e., the deposition of carbonaceous species on the catalyst and structural changes of the material, might account for the deactivation of the catalysts during the reduction of NO with propane and propene. As already described in Ref. [27] the formation of carbonaceous deposits depends markedly on the type of reducing agent and the reaction temperature. Generally, a higher concentration of carbonaceous deposits is formed with propene than with propane, which leads to a lower activity of the Ni-containing catalysts for the reduction of NO with propene.

During the reduction of NO with propane a decrease in the activity of the catalysts after the first cycle (from 150 to 600 °C) was observed for all three materials studied, while the activity between the second (600 to 150 °C) and the third cycle (150 to 600 °C) did not change. The intermediate oxidation of the catalysts at 600 °C in O_2, carried out between cycle 2 and 3, sufficiently removes coke species formed [17,22]. The treatment should, therefore, restore the initial activity of the catalysts, if coke formation is the main reason for the deactivation. The activity of the catalysts during cycle 3, however, remained at the level of the second cycle, which indicates that irreversible changes of the catalyst (and not only carbon deposition) are the main reason for the catalyst deactivation after high temperature reactions.

The effect of the formation of carbonaceous species is demonstrated in the NO reduction experiments carried out for an extended time at 475 and 600 °C. After exposing Ni/ZSM-5 and Ni/MOR to the reaction mixture at 475 °C immediately after the activation, NO conversion levels of 88 and 68% were obtained. For Ni/ZSM-5 the NO conversion was higher compared to that obtained at 475 °C during the experiment performed by varying the temperature between 150 and 600 °C, i.e., 65%, (see Fig. 1B), which indicates that a partial deactivation (most likely through deposition of carbonaceous species) during such temperature variations is taking place. In contrast, for Ni/MOR the same NO conversion was observed in both experiments (see Figs. 1A and 3B), which confirms that the formation of carbonaceous species in Ni/MOR is lower compared to Ni/ZSM-5, due to the lower concentration of acid sites [26]. After 50 h of reaction at 475 °C the temperature was increased to 600 °C for 50 h and the NO conversion decreased for both catalysts. It is interesting to note that for Ni/ZSM-5 an induction period of 10 h was observed at 600 °C, during which the NO conversion increased from 42 to 59%. After changing the reaction temperature back to 475 °C both catalysts showed a lower activity compared to the first part of the experiment. For Ni/ZSM-5 the NO conversion decreased from 88 to 60%, due to a severe and irreversible deactivation of the catalysts. For Ni/MOR the NO conversion decreased only from 68 to 54% indicating that changes of the catalyst structure resulting from the reaction at 600 °C were smaller in comparison with Ni/ZSM-5.

During the NO reduction with propene the difference in activity during all three cycles was very small for the three catalysts investigated. Having already shown that the presence of carbonaceous species is the main reason for the lower activity of the catalysts compared to the NO reduction with propane [26], reversible formation of coke during the reaction is proposed. The oxidation treatment between cycle 2 and 3 is concluded to remove the coke species formed. During the third reaction cycle, however, the formation of carbonaceous species occurs in a similar extent as during the first cycle and, therefore, the activity of the catalysts during the first and third cycle is the same for Ni/ZSM-5 and Ni/MCM-22. For Ni/MOR the activity during the second

and third cycle was the same, but it decreased after the first cycle, which indicates that structural changes of the catalysts already occurred during the first reaction cycle.

As shown in Ref. [26] the type and strength of the acid sites significantly influence the activity of the catalyst for the NO reduction with propane. Therefore, the decrease in the activity observed during the reaction at high temperatures is attributed partly to the removal of Brønsted acid sites resulting from the partial dealumination of the zeolites. In addition, Al^{3+} located in the zeolite framework acts as anchor for the Ni-ions. Thus, dealumination additionally leads to enhanced formation of Ni-oxide clusters within the zeolite pores.

For all samples, the formation of extraframework Al-oxide species was detected by IR spectroscopy and by ^{27}Al-NMR. After the reaction an intense IR band assigned to OH groups on extra-framework Al-oxide species was observed, which was only weakly intense in the fresh samples. Note that a small fraction of Al present in octahedral positions in the fresh Ni/MCM-22 and Ni/MOR was detected by ^{27}Al-NMR, while for Ni/ZSM-5 the signal at 0 ppm was not observed. After the reaction, octahedral Al species were detected in all catalysts (see Table 2). The highest concentration was observed in Ni/MOR after the reaction with propene and in Ni/MCM-22 after the reaction with propene and propane. Ion exchange positions in the investigated zeolites are occupied by protons and Ni^{2+} and Na^{+} ions. Note that Ni^{+} ions are formed only during the pretreatment done in vacuum to the samples before the CO adsorption experiments, and monovalent ions are not present under reaction conditions. The intensity of IR band at 3610 cm^{-1} (attributed SiOHAl groups) in the fresh sample decreased between 32 and 93% by catalysis at high temperatures. Comparing this decrease with the appearance of a small peak associated to octahedral Al in the ^{27}Al-NMR corresponding to a fraction of 2.4–6.1% of the total Al (see Table 2) suggests that the aluminum atoms associated to bridged hydroxyl groups are preferentially dealuminated.

The smallest difference in the IR spectra during CO adsorption between fresh and used samples was observed for Ni/MOR (see Table 3), which perfectly agrees with the minor decrease in activity observed during the NO reduction at 600 °C. For Ni/ZSM-5 and Ni/MCM-22 the intensity of the bands assigned to CO adsorption on monovalent Ni^{+} decreased significantly after reaction compared to the fresh catalysts ($> 60\%$). In general, the presence of CO interacting with monovalent Ni proves the existence of isolated Ni ions in the catalysts, because only isolated Ni^{2+} ions can be partially reduced to Ni^{+} by H_2O present in the zeolite structure [41,42]. This reaction can only occur during the activation of the catalysts in vacuum, while the formation of Ni^{+} is not expected under the reaction conditions of the NO_x reduction due to the presence of an excess of O_2. Therefore, the spectra of CO adsorption showing the disappearance of the band corresponding to CO interacting with Ni^{+} indicates that the deactivation Ni/ZSM-5 and Ni/MCM-22 during the reaction at 600 °C results from a decrease in the availability of isolated Ni ions.

The migration of Ni from isolated ion exchange positions into larger Ni-oxide species was followed by EXAFS. In the fresh catalysts Ni was present as Ni^{2+} at ion exchange positions as indicated by the number of O neighbors of around 3 and the minor Ni–Ni contributions ($N_{\mathrm{Ni-Ni}} \sim 0.7$). The minor extent of Ni–Ni contributions might indicate the presence of Ni^{2+} ions on cation sites next to each other surrounded by oxygen atoms of the zeolite framework. Similar structures have been observed previously for Ni-exchanged Y zeolite prepared by solid-state ion exchange [44]. Note that the contributions of the closest oxygen neighbors are only weakly affected by the formation of Ni-oxide species. It is not possible to differentiate between the contributions to the EXAFS from oxygen atoms from the zeolite lattice and from Ni-oxide clusters, while the presence of next nearest Ni neighbors unequivocally demonstrates the existence of Ni-oxide species. For the Ni/MOR and Ni/ZSM-5 catalysts the increase in the Ni–O and Ni–Ni coordination numbers suggests the formation of Ni-oxide particles. However, for Ni/MCM-22, which did not show such an increase, it is concluded that the Ni ions remain on ion exchange positions after the NO reduction at 600 °C. The lower intensity of the band assigned to CO adsorption on Ni^{+} on Ni/MCM-22 after reaction indicates that changes associated with the metal ions occurred, which are tentatively attributed to the migration of Ni ions to exchange positions not accessible for sorption of CO. Therefore, it is speculated that these Ni species are also not active for the NO_x reduction.

The position of the X-ray absorption edge depends on the effective charge density of the adsorbing atom and reflects the tendency of an atom to bind the electrons [45]. The position of the Ni K-edge of the fresh and used samples was 2.7 and 3.8 eV higher than that of reduced Ni. For the fresh samples the same position as for NiO was observed indicating that Ni was in an oxidation state of $+2$ in the Ni-exchanged zeolites. Conceptually, the further increase in the edge energy of the used sample compared to NiO indicates the coordination of Ni to a strongly electronegative neighbor. This could either be one of the reactants [46] or, more likely, O atoms in a Ni aluminate phase formed by the reaction of Ni with the extraframework Al-oxide species resulting from dealumination. Note that in $NiAl_2O_4$ the binding energy of the Ni $2p_{3/2}$ state (857 eV) is 3 eV higher than in NiO (854 eV) [46,47]. However, the increase of the Al in octahedral positions observed by NMR and the simultaneous appearance of the Ni–Ni contributions resulting from the formation of Ni-oxide clusters in the EXAFS on the Ni/MOR and Ni/ZSM-5 samples presents only an indirect indication of a relation between the dealumination and the Ni-oxide cluster formation.

In summary, all experiments indicate that the reduction of NO with propane and with propene in the presence of an excess of oxygen causes structural changes of the Ni-exchanged zeolites. These changes can be differentiated into

(i) reversible changes resulting from the deposition of carbonaceous species and (ii) irreversible changes such as the dealumination of the zeolite and the migration of Ni. For Ni/MOR Ni-oxide clusters of 8.0 and 7.0 Å size are formed during the reduction of NO with propene and propane but the accessibility of Ni for the reactants decreased only ∼ 30%. Therefore, this catalyst was only slightly deactivated under reaction conditions. For Ni/ZSM-5 a part of Ni migrates and forms Ni-oxide clusters of 7.4 and 6.5 Å size, resulting in a decreased accessibility of active sites of 57 and 72% during the reduction of NO with propene and propane. For Ni/MCM-22, a decrease in the accessibility by 67% indicates that Ni migrates to positions where it is more difficult to be accessed under reaction conditions. Formation of NiO clusters was not observed for this material. Dealumination observed from the increase or appearance of a fraction of Al located in octahedral positions by ^{27}Al-NMR might cause the migration of Ni in the three cases.

5. Conclusions

It was clearly shown that the chemical state of Ni^{2+}, i.e., as isolated ions on ion exchange positions or Ni^{2+} on the surface of small Ni-oxide clusters, affects the activity to a less significant extent compared to the changes in the location of Ni within the zeolite framework, which directly influences the accessibility for the reactants. Changes in the activity of Ni-exchanged zeolites were observed after the reduction of NO with propane and propene. The main reasons for such changes are related to (i) the deposition of carbonaceous species on the catalysts and (ii) structural changes associated to Ni and Al.

The effects of the deposition of carbonaceous species on the catalytic surface were more pronounced for those materials that contained a higher concentration of acid sites. A significant increase in the NO conversion was observed for Ni/ZSM-5 exposed to the reaction mixture at 475 °C directly after activation, in comparison with the conversion obtained at 475 °C for a sample that has been exposed to the reaction mixture while varying temperatures between 150 and 600 °C, since the formation of the carbonaceous species is the highest at temperatures below 475 °C.

In the fresh materials, Ni is present as Ni^{2+} ions located in ion exchange positions in Ni/MOR, Ni/ZSM-5, and Ni/MCM-22. Dealumination of the samples due to their exposure to the reaction mixtures at high temperatures caused the decrease of accessible Ni ions. For Ni/ZSM-5 and to a lower extent for Ni/MOR the decrease in the accessibility of Ni resulted from the formation of Ni-oxide clusters, while for Ni/MCM-22 Ni ions migrated to less accessible positions. In all cases, the reduced accessibility accounts for the decrease in the catalytic activity.

Acknowledgments

The authors acknowledge the staff of the beamline X1 (Dr. N. Haack, Dr. E. Welter, and M. Herrmann) at Hasylab DESY, Hamburg, Germany for their kind help. Special thanks to J.O. Barth and R.Q. Su for the NMR measurements.

This work was supported by STW/NWO, The Netherlands, under Project 326-710 and has been performed under the auspices of NIOK and PIT.

References

[1] X. Wang, H.Y. Chen, W.M.H. Sachtler, Appl. Catal. B 26 (2000) L227.
[2] Y. Li, J.N. Armor, Appl. Catal. B 3 (1993) L1.
[3] Y. Li, J.N. Armor, Appl. Catal. B 2 (1993) 239.
[4] S.E. Maisuls, K. Seshan, S. Feast, J.A. Lercher, Appl. Catal. B 29 (2001) 69.
[5] X. Feng, W.K. Hall, Catal. Lett. 41 (1996) 45.
[6] X. Feng, W.K. Hall, J. Catal. 166 (1997) 368.
[7] T.V. Voskoboinikov, H.Y. Chen, W.M.H. Sachtler, Appl. Catal. B 19 (1998) 279.
[8] H.Y. Chen, T. Voskoboinikov, W.M.H. Sachtler, J. Catal. 180 (1998) 171.
[9] H.Y. Chen, T. Voskoboinikov, W.M.H. Sachtler, Catal. Today 54 (1999) 483.
[10] F. Witzel, G.A. Sill, W.K. Hall, J. Catal. 149 (1994) 229.
[11] Y. Traa, B. Burger, J. Weitkamp, Micropor. Mesopor. Mat. 30 (1999) 3.
[12] Y. Li, J.N. Armor, J. Catal. 150 (1994) 376.
[13] D. Kaucký, A. Vondrová, J. Dedecek, B. Wichterlová, J. Catal. 194 (2000) 318.
[14] Z. Sobalik, J. Dedecek, D. Kaucký, B. Wichterlová, L. Drozdova, R. Prins, J. Catal. 194 (2000) 330.
[15] Z. Chajar, V. Le Chanu, M. Primet, H. Praliaud, Catal. Lett. 52 (1998) 97.
[16] P. Marturano, L. Drozdova, A. Kogelbauer, R. Prins, J. Catal. 192 (2000) 236.
[17] J.L. d'Itri, W.M.H. Sachtler, Appl. Catal. B 2 (1993) L7.
[18] A. Giroir-Fendler, P. Denton, A. Boreave, H. Praliaud, M. Primet, Top. Catal. 16/17 (2001) 237.
[19] P. Denton, A. Giroir-Fendler, H. Praliaud, M. Primet, J. Catal. 189 (2000) 410.
[20] C.E. Quincoces, A. Kikot, E.I. Basaldella, M.G. Gonzalez, Ind. Eng. Chem. Res. 38 (1999) 4236.
[21] Y. Li, P.J. Battavio, J.N. Armor, J. Catal. 142 (1993) 561.
[22] J.O. Petunchi, W.K. Hall, Appl. Catal. B 3 (1994) 239.
[23] Z. Li, M. Flytzany-Stephanopoulos, Appl. Catal. B 22 (1999) 35.
[24] M. Lezcano, A. Ribotta, E. Miro, E. Lombardo, J.O. Petunchi, C. Moreaux, J.M. Dereppe, J. Catal. 168 (1997) 511.
[25] J.Y. Yan, G.-D. Lei, W.M.H. Sachtler, H.H. Kung, J. Catal. 161 (1996) 43.
[26] B.I. Mosqueda-Jiménez, A. Jentys, K. Seshan, J.A. Lercher, submitted to J. Catal. (2003).
[27] B.I. Mosqueda-Jiménez, A. Jentys, K. Seshan, J.A. Lercher, Appl. Catal. B, in press, doi: 10.1016/S0926-3373(02)00280-1.
[28] T.J. Ressler, Physique IV 7 (1997) C2.
[29] A.L. Ankudinov, J.J. Rehr, Phys. Rev. B 62 (2000) 2437.
[30] A.L. Santos Marques, J.L. Fontes Monteiro, H.O. Pastore, Micropor. Mesopor. Mat. 32 (1999) 131.
[31] S.L. Lawton, A.S. Fung, G.J. Kennedy, L.B. Alemany, C.D. Chang, G.H. Hatzikos, D.N. Lissy, M.K. Rubin, H.K.C. Timken, S. Steuernagel, D.E. Woessner, J. Phys. Chem. 100 (1996) 3788.

[32] W. Kolodziejski, C. Zicovich-Wilson, C. Corell, J. Perez-Pariente, A. Corma, J. Phys. Chem. 99 (1995) 7002.
[33] P. Meriaudeau, V.A. Tuan, V.T. Nghiem, F. Lefevbre, V.T. Ha, J. Catal. 185 (1999) 378.
[34] M. Stockenhuber, J.A. Lercher, Micropor. Mater. 3 (1995) 457.
[35] A. Jentys, A. Lugstein, H. Vinek, J. Chem. Soc., Faraday Trans. 93 (1997) 4091.
[36] F. Moreau, P. Ayrault, N.S. Gnep, S. Lacombe, E. Merlen, M. Guisnet, Micropor. Mesopor. Mat. 51 (2002) 211.
[37] V.L. Zholobenko, M.A. Makarova, J. Dwyer, J. Phys. Chem. 97 (1993) 5962.
[38] K. Hadjiivanov, H. Knözinger, M. Hihaylov, J. Phys. Chem. B 106 (2002) 2618.
[39] L. Bonneviot, F.X. Cai, M. Che, M. Kermarec, O. Legendre, C. Lepetit, D. Olivier, J. Phys. Chem. B 91 (1987) 5912.
[40] M. Kermarec, D. Olivier, M. Richard, M. Che, F. Bozon-Verduraz, J. Phys. Chem. B 86 (1982) 2818.
[41] P.H. Kasai, R.J.J. Bishop, D.J. McLeod, J. Phys. Chem. 82 (1978) 279.
[42] A.M. Prakash, L. Kevan, J. Phys. Chem. 100 (1996) 19587.
[43] H. Choo, S.B. Hong, L. Kevan, J. Phys. Chem. B 105 (2001) 1995.
[44] H. Förster, U. Hatje, Solid State Ionics 101 (1997) 425.
[45] A. Tadjeddine, A. Lahrichi, G. Tourillon, J. Electroanal. Chem. 360 (1993) 261.
[46] J. Blanco, P. Avila, J.L.G. Fierro, Appl. Catal. A 96 (1993) 331.
[47] M. Lenglet, F. Hochu, J. Durr, M.H. Tuilier, Solid State Commun. 104 (1997) 793.